Polymer Chemistry

Accepted Manuscript

ROYAL SOCIETY OF CHEMISTRY

www.rsc.org/polymers

Table of Contents

Enhancing melt stability of polylactide stereocomplexes by using solid-state cross-linking strategy during melt-blending process

Hongwei Bai[†‡], Huili Liu[†], Dongyu Bai[†], Qin Zhang[†], Ke Wang[†], Hua Deng[†], Feng Chen[†], Qiang Fu[†]*

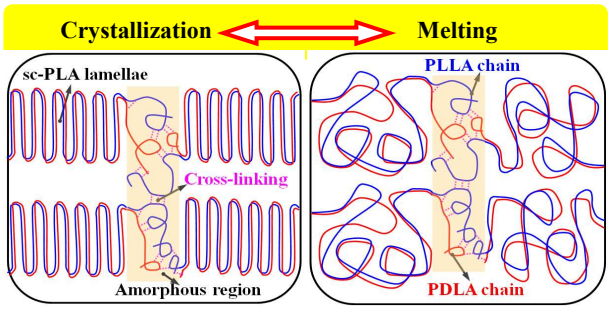

Selective cross-linking of PLLA and PDLA chain couples in amorphous phase allows for the formation of stereocomplex (sc) crystallites in continuous melting and recrystallization process to be perfectly reversible.

Enhancing melt stability of polylactide stereocomplexes by using solid-state cross-linking strategy during melt-blending process

Hongwei Bai[†‡], *Huili Liu*[†], *Dongyu Bai*[†], *Qin Zhang*[†], *Ke Wang*[†], *Hua Deng*[†], *Feng Chen*[†], *Qiang Fu*[*†]

[†]College of Polymer Science and Engineering, State Key Laboratory of Polymer Materials Engineering, and [‡]College of Light Industry, Textile and Food Engineering, Sichuan University, Chengdu 610065, P. R. China

Abstract: Stereocomplexation between poly(L-lactide) (PLLA) and poly(D-lactide) (PDLA) provides a feasible route for improving the performance of polylactide (PLA), including mechanical strength, thermal stability and hydrolysis resistance. In recent years, several effective methods have been developed to prepare polylactide stereocomplexes (sc-PLA) from commercial available, linear, high-molecular-weight PLLA and PDLA. However, it is still a big challenge to attain pure sc-PLA in the melt-processed products because the prepared sc-PLA has a very poor melt stability, namely, the ability to trigger the reformulation of stereocomplex (sc) crystallites after complete melting is significantly depressed, resulting in a formation of mixed

[*] Corresponding author. Tel./Fax: +86 28 8546 1795. E-mail: qiangfu@scu.edu.cn (Q. Fu).

homochiral (hc) and sc crystallites. Here we present a facile strategy to fabricate sc-PLA with good melt stability by low-temperature (180 ℃) melt-blending of equimolar PLLA and PDLA in the presence of trace amount (0.1-0.5 wt%) of cross-linker. During the blending process, sc crystallites form rapidly, followed by a slight cross-linking of PLLA and PDLA chain couples in mobile amorphous phase, whereas the chain couples in crystalline phase hardly participate in the cross-linking reaction. The exclusive cross-linking of PLAs chains in amorphous phase not only allows for the introduction of abundant cross-linking points at the ends of the chain couples to prevent them from completely decoupling upon melting but also retains large amounts of long crystallizable PLAs segments existed in the initially formed sc crystallites to impart the resulting sc-PLA with an excellent recrystallization ability upon cooling. The formation or reformulation of sc crystallites in the continuous melting and recrystallization process is found to be perfectly reversible, without any trace of hc crystallites.

1. Introduction

Nowadays, developing bio-based polymers to replace conventional petroleum-based polymers has received considerable attention with the growing awareness of sustainability.[1, 2] Polylactide (PLA), as one of the most promising bio-based polymers derived from renewable resources such as corn and sugarcane, exhibits a great potential as an eco-friendly alternative in a wide variety of applications from biomedical materials to industrial packaging materials because of its excellent biocompatibility, nontoxicity, favorable biodegradability, extraordinary transparency, good mechanical strength, and easy processability.[3-6] However, in comparison with generally used engineering plastics such as poly(butylene terephthalate) (PBT), both the inferior thermal resistance to deformation limited by the relatively low melting temperature (150-180 ℃,

depending on the optical purity and molecular weight[7, 8]) and the poor long-term performance caused by the degradation during its service life make PLA less competitive in the market. Even in some biomedical applications, an improvement in the heat resistance of PLA is indispensable to avoid deformation after steam sterilization (135 ℃, high steam pressure) and dry heat sterilization (160-190 ℃).[9, 10] Stereocomplexation between enantiomeric poly(L-lactide) (PLLA) and poly(D-lactide) (PDLA) provides a feasible and robust route to simultaneously improve the heat resistance and the durability of PLA so as to fulfill the essential requirements in various industrial applications.[11-15] PLA stereocomplexes (sc-PLA) formed by blending of equimolar PLLA and PDLA have a much higher melting temperature (230 ℃) and a far better hydrolysis resistance as compared with homocrystallized PLLA or PDLA.[11-13] The highest heat distortion temperature (HDT) for sc-PLA is over 200 ℃, while HDT for highly crystalline PLA is only 100-120 ℃.[14]

The physicochemical properties of sc-PLA strongly rely on the level of crystallinity. Thus, enhancing stereocomplex crystallization becomes a matter of concern.[16-21] Up to now, extensive efforts has been devoted to develop useful preparation methods, such as supercritical fluid technology[16] and annealing[17, 18], for improving the efficiency of stereocomplex formation. Recently, Bao et al.[19] proposed a simple but effective approach to generating pure sc-PLA by melt-blending enantiomeric PLAs at low temperatures (160-210 ℃) where only stereocomplex (sc) crystallites can grow but the homochiral (hc) crystallites cannot form. High molecular weight ($M_w \geq 10^5$) is generally believed to a prerequisite for achieving high performance of sc-PLA. However, sc-PLA has a weak melt memory to re-form sc crystallites after complete melting and the ability of restoring sc-PLA decreases with increasing molecular weight.[22, 23] When pure sc-PLA are melted and crystallized again, hc crystallization always prevails over the

sc crystallization, leading to a coexistence of hc crystallites and sc crystallites in the melt-processed, high-molecular-weight PLLA/PDLA (50/50) blend.[22-24] Therefore, it is an extremely challenging task to prepare stereocomplexed PLA products with good melt stability from linear high-molecular-weight PLAs by using industrially meaningful melt-processing technology. Fukushima et al.[25] attempted to use multi-block copolymer of PLLA and PDLA as a compatibilizer to overcome the melt instability and thus enhance the reformulation of sc crystallites after melting of the blend. However, the copolymer can depress the concomitant hc crystallization, but the exclusive formation of sc crystallites cannot be easily achieved. On the other hand, several PLA architectures have been applied to improve the melt-stability of sc-PLA.[26-31] For example, the formation of well-stereocomplexed crystallites is found to be complete and perfectly reversible in the melt-crystallization of star-shaped enantiomeric PLAs and linear stereoblock PLAs due to the hard-lock-type interactions and the neighboring effect of the stereo-regular sequences, respectively.[26, 29] Nevertheless, a tedious and complex process is required to synthesize these polymers with special structures, which significantly limits their utility in large-scale industrial applications at present, so there is a current growing interesting in developing an economic and facile strategy to fabricate sc-PLA with excellent melt stability from commercial available, linear, high-molecular-weight PLAs.

Solid-state modification (SSM), such as solid-state polycondensation traditionally used for increasing molecular weight of semicrystalline polyester, refers to a process of selectively modifying amorphous phase of semicrystalline polymers.[30, 32] Because it is generally carried out at a temperature between the melting temperature (T_m) and the glass-transition temperature (T_g) of the polymer, the SSM allows for the exclusive modification of the chain structures in the mobile amorphous phase, whereas the chain segments in the rigid crystalline phase do not

participate in the reactions. Inspired by the idea of SSM to selectively modify amorphous phase, herein, we propose a facile strategy to achieve high stereocomplexation with good melt stability from linear high-molecular-weight PLAs by combining low-temperature (180 ℃) melt-blending and solid-state cross-linking (SSC) technologies. It is expected that pure sc crystallites could be formed rapidly during the melt-blending process, and the subsequent cross-linking of mobile PDLA and PLLA chain couples in amorphous phase of the initially formed sc crystallites could prevent them from decoupling in melt state and promote them arrange in a side-by-side manner at the crystallization frontier. Because the blending temperature is just located in the temperature window (about 50 ℃ below the T_m of sc-PLA but well above its T_g) required for SSC and the formation of sc crystallites is much faster than the dicumyl peroxide (DCP) initiated cross-linking reaction (Scheme 1) between PLAs chains and triallyl isocyanurate (TAIC), both the formation of sc crystallites and the subsequent cross-linking of mobile PLAs chain couples have been successfully realized in one-step melt-blending process by taking advantage of the wide time window and the appropriate temperature window. Influence of cross-linking on the melt stability of sc-PLA was investigated. And, the thermomechanical properties of the well-stereocomplex PLAs obtained by slight cross-linking were also highlighted by comparing with those of highly crystalline PLLA. This work could open a new way to rapidly fabricate sc-PLA with controllable melt stability by using simple melt-blending technology, without any further purification step and special processing equipment.

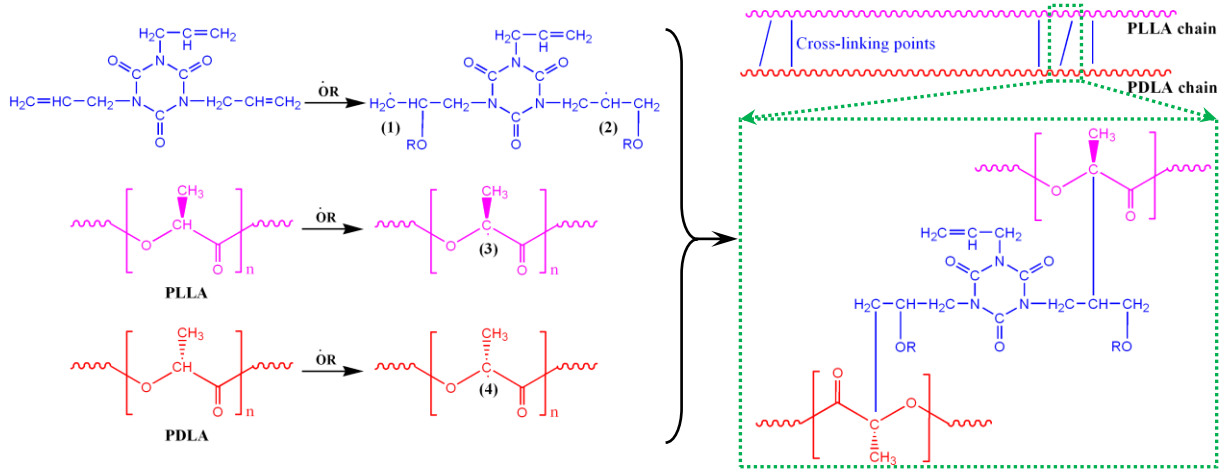

Scheme 1. Reaction mechanism for chemical cross-linking of enantiomeric PLAs with DCP and TAIC.

2. Experimental Section

2.1 Materials

Commercial poly(L-lactide) (PLLA, grade 4032D, D-isomer = 1.2-1.6%, M_w = 170000 g mol-1) was purchased from NatureWorks LLC, U.S.A. Poly(D-lactide) (PDLA, D-isomer = 99.5%, M_w = 120000 g mol^{-1}) was kindly supplied by Zhejiang Hisun Biomaterial Co. Ltd., China. Dicumyl peroxide (DCP) used as a radicals initiator and triallyl isocyanurate (TAIC) used as a cross-linker were supplied by Sinopharm Chemical Reagent Co., Ltd., China. Hexafluoroisopropanol (HFIP) and other chemical reagents were obtained from Aladdin Industrial Inc. (Shanghai, China).

2.2 Sample preparation

PLLA/PDLA (50/50) blend without and with various concentrations of DCP (0.3 wt%) and TAIC (0.1, 0.2, 0.3, and 0.5 wt%) were prepared using a Haake Rheomix 600 internal mixer (Germany) at a temperature of 180 ℃ and a rotor speed of 60 rpm for 5 min. The obtained

samples were denoted as a code of LD-*x*, where *x* represents the weight percentage of TAIC in the blend. For comparison, PLLA without and with cross-linker (coded as PLLA-*x*) were also processed with the same procedure. Both PLLA and PDLA were dried overnight in a vacuum oven at 60 ℃ prior to use. Specially, to achieve precise loading and good dispersion of trace amounts of radicals initiator and cross-linker in the PLLA and PLLA/PDLA blend, both DCP and TAIC was firstly dissolved in dry ethanol and then mixed with the granules of PLAs before the melt-blending. During the entire blending period, the evolution of torque with blending time was recorded in order to detect the stereocomplex formation and the cross-linking reaction. The specimens of LD-*x* used for mechanical testing were fabricated using a HAAKE MiniJet II injection molder (Germany) at a barrel temperature of 250 ℃ under a dry nitrogen flow. The mold temperature was determined according to the crystallization temperature of each sample. For convenience, the injection molded samples were designated as PLLA-*x*@*y* and LD-*x*@*y*, where *y* indicates the mold temperature.

2.3 Characterizations and measurements

The gel fraction in the cross-linked samples was estimated by the weight percentage of insoluble gel in HFIP using the following equation:

$$\text{Gel fraction } (\%) = (W_g / W_0) \times 100 \qquad (1)$$

where W_0 and W_g are the dried weights of initial cross-linked specimen and remaining gel component after dissolving in HFIP at room temperature for 48 h, respectively.

The obtained dried gel can reach the equilibrium state of swelling after immersion in HFIP again for 48 h at room temperature. The degree of swelling (volume ratio of absorbed HFIP solvent to dried gel) was calculated as following:

$$\text{Degree of swelling } = [(W_s - W_g) / W_g](\rho_p / \rho_{HFIP}) \qquad (2)$$

where W_g is the weight of dried gel, W_s is the weight of swollen gel in HFIP; ρ_p and ρ_{HFIP} are the densities of PLA and HFIP, respectively.

The structural changes involved in the cross-linking reaction were examined using a Thermo Nicolet 3700 spectrometer (U.S.A.) equipped with an attenuated total reflectance (ATR) accessory. Fourier transform infrared spectroscopy (FT-IR) spectra were collected by adding 32 scans at a resolution of 4 cm^{-1}. For each cross-linked sample, the dry gel prepared by extracting with HFIP was used for the FT-IR measurement.

Thermal analysis was performed on a Perkin-Elmer pyris-1 differential scanning calorimeter (DSC, U.S.A.) at heating/cooling rates of 10 ℃/min in the temperature range of 30 ℃ to 250 ℃. For each specimen, the DSC nonstop cycle was repeated four times under a dry nitrogen atmosphere to highlight the stability of observed thermal properties. To ensure the reliability of data obtained, high-purity indium was used as standard to calibrate the heat flow and temperature before the measurements.

Crystalline structure was analyzed using a Philips X'Pert pro MPD diffractometer with a CuKα radiation. The wide-angle X-ray diffraction (WAXD) spectra were recorded at 40 kV and 40 mA with a scanning angle from 10° to 40°. The crystallinity of homochiral crystallites ($X_{c,hc}$), stereocomplex crystallites ($X_{c,sc}$), and overall crystallites (X_c) can be evaluated from WAXD profiles according to the method reported by Tsuji et al[33].

Dynamic mechanical analysis (DMA) was performed on a TA Q800 equipment (U.S.A.) in a single-cantilever mode with a sinusoidal oscillating strain of 10 μm and a frequency of 1 Hz. Dynamic storage modulus (G') was measured from 0 to 200 ℃ at a heating rate of 3 ℃/min. To ensure the reproducibility of results obtained, two independent specimens were tested for each sample.

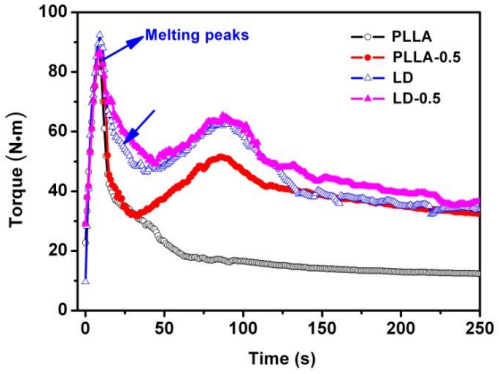

Figure 1. Torque-time curves for the melt blending of PLLA and PLLA/PDLA blend with and without 0.5 wt% TAIC at 180 ℃.

3. Results and Discussion

3.1 Stereocomplex formation and cross-linking

Torque-time curves can be used to explore the structural change of polymers during melting or melt-blending in a torque rheometer.[34, 35] If there is a strong interaction between polymer chains, a relatively high torque value will be observed in the torque-time curves. Figure 1 shows the torque evolution with time during melting of PLLA and blending of equimolar PLLA and PDLA in the presence of cross-linker. The first sharp and strong peak in each curve is the melting peak of PLA pellets. For pure PLLA, the torque value drops rapidly with the melting of PLLA pellets and then reaches a stable plateau. However, with the introduction of 0.5 wt% TAIC into PLLA, a substantial enhancement in torque is noted after the melting peak, confirming the occurrence of chemical cross-linking reactions between PLLA and TAIC. Similar tendency can also be seen in the torque-time curve of PLLA/PDLA blend. The notable increase in torque after the melting peak has been demonstrated to be associated with the stereocomplex formation.[35] Very interestingly, the level of torque for PLLA with 0.5 wt% TAIC is found to be comparable to that for pure PLLA before the onset of the cross-linking reactions (Figure 1), but PLLA/PDLA blend

exhibits a much higher torque in this situation (as highlighted by the arrow) because of the much slower decrease in torque with the melting of PLAs pellets. This result indicates that the stereocomplex formation proceeds much more quickly than the cross-linking reactions. As soon as part of PLAs pellets are melted during the melting process, the stereocomplextion between the mobile PLLA and PDLA chains occurs immediately under the drive of strong shear stress in the internal mixer. Because the cross-linking network can only be introduced into the amorphous regions of semicrystalline polymers,[36] the big time lag between the formation of sc crystallites and the onset of cross-linking reactions provides a good chance for the exclusive cross-linking of PLLA and PDLA chain couples located in the mobile amorphous phase of the preformed sc crystallites. Unexpectedly, no evident difference in the evolution of torque with time can be observed in PLLA/PDLA blend with 0.5 wt% TAIC as compared with PLLA/PDLA blend, suggesting that no noticeable cross-linking reactions occur when a small amount of cross-linker is added into the blend. The appearances of the as-prepared samples are given in Figure 2. Clearly, the final shapes of the melt-processed PLLA and PLLA/PDLA blend are glassy solids hard to make into powders (Figure 2a and b) and powdery crystallites (Figure 2c and d), respectively, independent of the presence of cross-linker. WAXD analysis provides clear evidence for the exclusive formation of sc crystallites in both the PLLA/PDLA blend without and with various amounts of TAIC. As shown in Figure 3, the WAXD profiles of the blends show three characteristic diffraction peaks of sc crystallites at around 12.0 °, 20.9 °, 24.0 °, corresponding to the (110), (300)/(030), and (220) planes, respectively,[13] but no characteristic peaks of usually observed α-form hc crystallites at around 14.8 °, 16.9 °, 19.0 ° and 22.5 °, assigned to the (010), (200)/(110), (203), and (210) planes, respectively,[37] can be detected.

Figure 2. Appearance of (a) PLLA, (b) cross-linked PLLA, (c) PLLA/PDLA blend, and (d) cross-linked PLLA/PDLA blend.

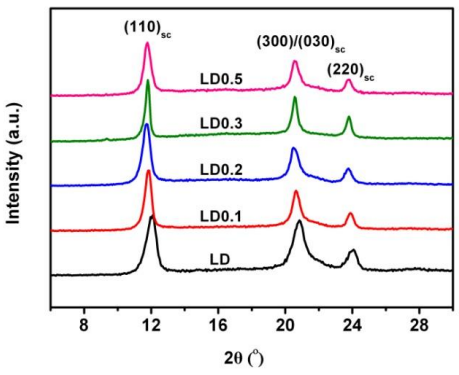

Figure 3. WAXD profiles of as-prepared PLLA/PDLA blend with various amounts of TAIC.

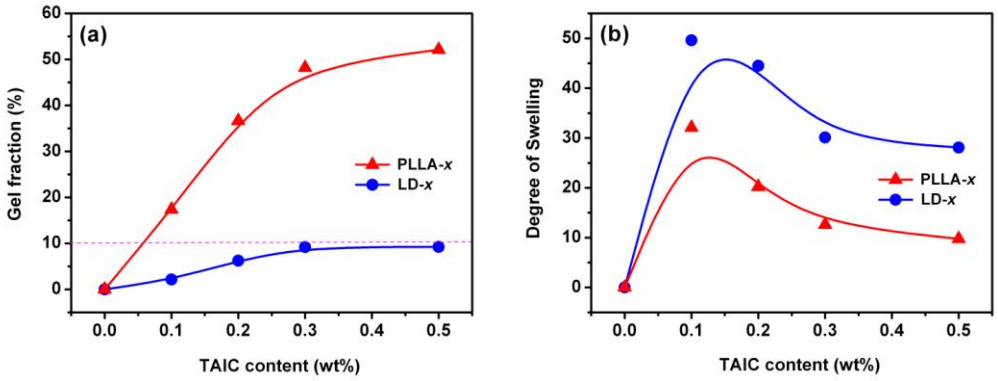

Figure 4. (a) Gel fraction and (b) swelling degree of cross-linked PLLA and PLLA/PDLA blend as a function of TAIC concentration.

Considering that the torque may become less sensitive to the structural changes induced by the cross-linking reactions when large amounts of powdery sc crystallites are rapidly formed in the melt of PLLA/PDLA blend, the gel fraction and swelling degree were measured to clarify whether the cross-linking reactions occurs in the blend during the melt-blending process as expected. Figure 4a compares the changes in gel fraction of PLLA and PLLA/PDLA blend with increasing TAIC concentration from 0.1 wt% to 0.5 wt%. The gel fraction of PLLA increases dramatically from 17.4 % to 48.2 % with the TAIC concentration up to 0.3 wt% and then levels off. However, blending PLLA with equimolar PDLA gives rise to a much lower extent of cross-link reactions and the maximum gel fraction is only 9.2 %, clearly indicating that the formation of sc crystallites in the melt can distinctly depress the cross-linking reactions because of the rapid decrease in the volume fraction of amorphous phase and thus only small amounts of cross-linking structures are formed between mobile PLAs chains and TAIC molecules. On the other hand, in comparison with PLLA, PLLA/PDLA blend exhibits a looser cross-linking

network after being cross-linked, as evidenced by the reduced swelling capacity of the obtained gel (Figure 4b).

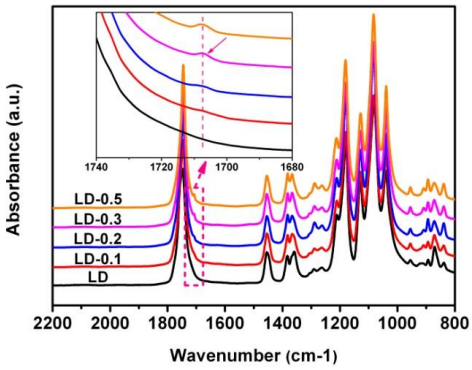

Figure 5. FT-IR absorption spectra of PLLA/PDLA blend with various amounts of TAIC.

In order to gain insight into the structural changes involved in the cross-linking reactions, FT-IR absorbance spectra of PLLA/PDLA blend with different amounts of TAIC were recorded and results in the range of 800-2200 cm^{-1} are presented in Figure 5. The strong peak at 1747 cm^{-1} is associated with the carbonyl vibration of PLA. Before the FT-IR measurements, the cross-linked blend was purified by HFIP extraction to remove free PLAs chains and possible residual TAIC. When compared with un-cross-linked blend, one noticeable feature in the spectra of the cross-linked blend is the appearance of a weak shoulder peak (as indicated by the arrow) attributed to the carbonyl group of TAIC at about 1705 cm^{-1},[38] implying the occurrence of cross-linking reactions between PLAs chains and TAIC molecules. Moreover, the peak intensity (can be regarded as an indicator of cross-linking density) increases with increasing TAIC concentration, which is consistent with the gradually decreased swelling degree (Figure 3b). The cross-linking reaction between PLA and TAIC in the presence of DCP has been discussed in the literature.[38] It is generally believed that DCP can decompose into cumyl radicals in PLA melt to initiate the macro-radicals in the backbone of PLA and the double bonds of allyl groups in TAIC

can easily break into monomer radicals at the same time, consequently, the cross-linking structures are generated by radicals reaction between PLA and TAIC. In the present study, the radical reaction between hetero-chiral PLAs chain couples and TAIC molecules is more likely to happen as compared to that between homo-chiral PLA and TAIC because the stereocomplex crystallization could promote the major fraction of PLLA and PDLA chains interact with each other in amorphous phase. The cross-linking reaction mechanism is given in Scheme 1.

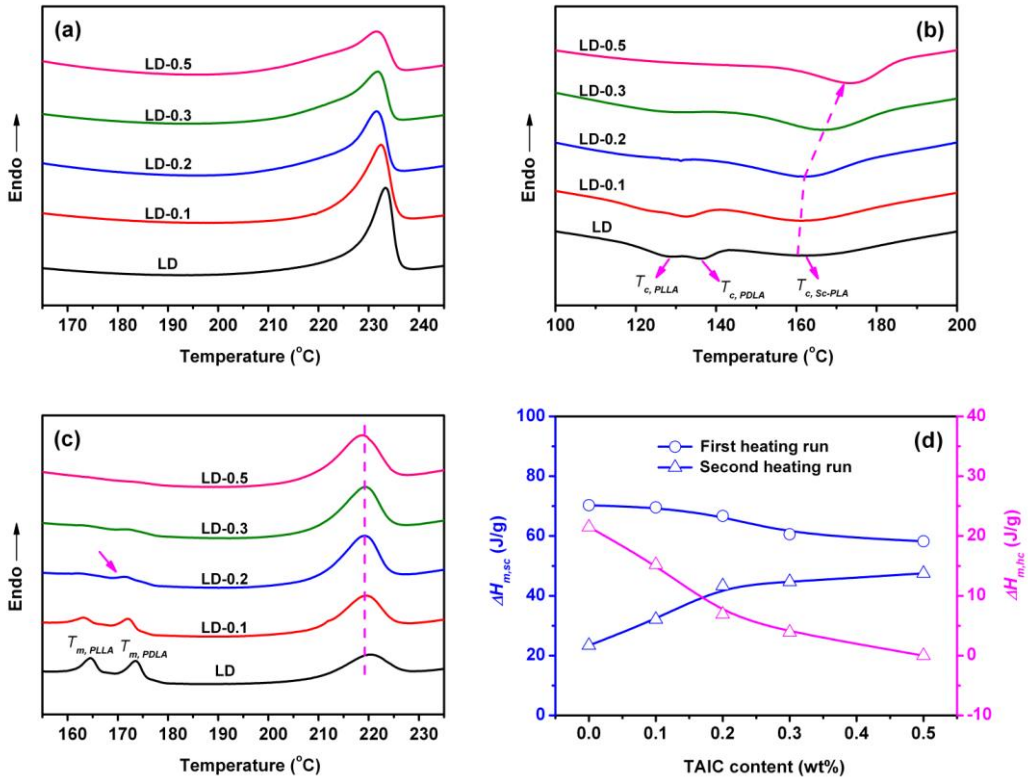

Figure 6. DSC thermograms of PLLA/PDLA blend with and without TAIC (a) during the first heating run, (b) during the cooling run after melting at 250 ℃ for 3 min, and (c) during the second heating run after melting recrystallization. The rate of heating and cooling was 10 ℃/min. (d) Melting enthalpies of sc crystallites ($\Delta H_{m,sc}$) and hc crystallites ($\Delta H_{m,hc}$) obtained in the DSC heating runs for PLLA/PDLA blend without and with various amounts of TAIC.

3.2 Melt stability

Melt stability of the melt-blended PLLA/PDLA (50/50) blend with and without cross-linking structures has been comparatively studied by DSC and WAXD. Figure 6a-c present the DSC thermograms of the blends and a summary of the DSC data are listed in Table S1 and Figure 6d. In the first heating scans, both the un-cross-linked blend and the cross-linked blends exhibit very similar thermograms, all showing only one strong melting peak characteristic of sc crystallites at around 231.5-233.5 ℃ (Figure 6a), further confirming the exclusive formation of sc crystallites without any trace of hc crystallites.

In the second heating scans after cooling to 30 ℃, three melting peaks, the one at 164.6 ℃ for PLLA, the second at 173.6 ℃ for PDLA, and the third at 220.0 ℃ for sc-PLA, are observed, indicating formation of a mixture of hc and sc crystallites (Figure 6c). In contrast to this, it is very interesting that increasing cross-linking extent gives rises to a substantial decrease in the melting enthalpy of hc crystallites ($\Delta H_{m,hc}$) as well as a remarkable enhancement in the melting enthalpy of sc crystallites ($\Delta H_{m,sc}$) (Figure 6d and Table S1), although the content of sc crystallites in the melt-blended PLLA/PDLA blend decreases apparently with increasing TAIC concentration up to 0.5 wt%, clearly demonstrating that the selective cross-linking of mobile PLAs chain couples can significantly enhance the ability of PLLA/PDLA blend to re-form sc crystallites from the melt as expected. The crystallization temperature for stereocomplex formation ($T_{c,sc}$) is between 160.6 ℃ and 173.7 ℃, depending on the cross-linking extent (Figure 6b). Particularly, the PLLA/PDLA blend cross-linked with 0.5 wt% TAIC gives only one sharp melting peak of sc crystallites at 218.5 ℃ (Figure 6c) and three main diffraction peaks of sc crystallites (Figure 7), suggesting an excellent melt stability of the blend. Meanwhile, the observed $\Delta H_{m,sc}$ (47.5 J/g) (Figure 6d and Table S1) is comparable to that of the sc crystallites

formed from well-defined star-shaped PLAs.[26] With regard to the decrease in $T_{m,sc}$ and $\Delta H_{m,sc}$ after melting and recrystallization (Table S1), it should be attributed to the two completely different formation conditions. The original sc crystallites prepared by melt-blending is formed under a strong shear field, whereas the recrystallized sc crystallites is obtained under a quiescent condition. The shear stress can drastically influence the crystallization of semicrystalline polymers, e.g., accelerating crystallization, increasing crystallinity, and improving crystalline perfection.[39] Most importantly, the good melt stability of sc crystallites formed in the cross-linked blend can be further verified by applying multiple DSC heating/cooling/heating thermal cycles in the temperature range of 30 ℃ to 250 ℃. As presented in Figure 8, the exclusive formation of sc crystallites is found to be perfectly reversible after melting and recrystallization. The values of $T_{c,sc}$, $T_{m,sc}$, and $\Delta H_{m,sc}$ remain constant in three thermal cycles. To the best of our knowledge, this is the first example of preparing sc-PLA with good melt stability from linear high-molecular-weight PLAs by selectively cross-linking amorphous phase during the melt-blending process.

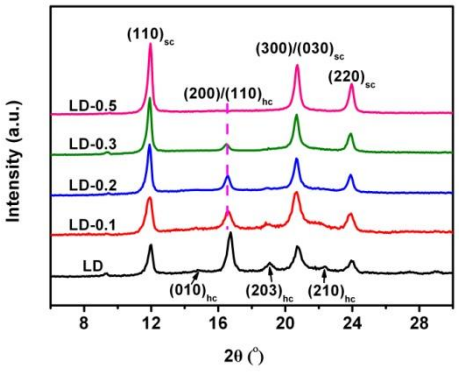

Figure 7. WAXD profiles of melt-recrystallized (cooling down to 30 ℃ at a rate of 10 ℃/min after melting at 250 ℃ for 3 min) PLLA/PDLA blend with various amounts of TAIC.

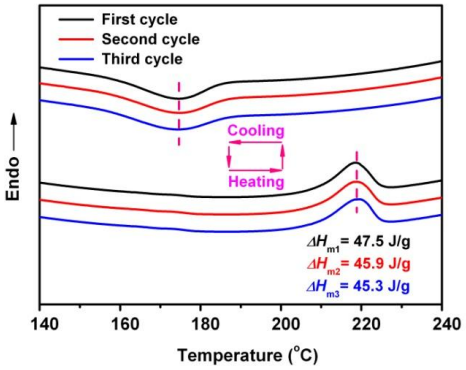

Figure 8. DSC thermograms of PLLA/PDLA blend with 0.5 wt% TAIC. The DSC nonstop cycle was repeated three times in the temperature range of 30 ℃ to 250 ℃ after eliminating thermal history at 250 ℃, and the rate of heating and cooling was 10 ℃/min.

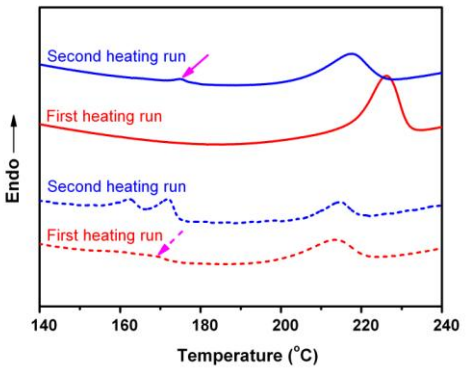

Figure 9. DSC thermograms of PLLA/PDLA blend cross-linked with 0.5 wt% TAIC (solid line) and c-PLLA/c-PDLA blend (dashed line) during first heating run and during second heating run after melting recrystallization at a rate of 10 ℃/min.

To further make it clear whether the selective cross-linking is the main contributor for the inspiring enhancement in the melt stability, other two different samples were prepared. Figure 9

shows the DSC thermograms of the obtained samples. It is very interesting to find that, after melting and recrystallization, the sc crystallites are almost exclusively formed in the blend prepared by cross-linking of pre-prepared PLLA/PDLA blend with 0.5 wt% TAIC. Formation of a few hc crystallites may be caused by the insufficient diffusion of TAIC molecules into the amorphous phase of the sc crystallites with high crystallinity due to the time limitation during the blending process. In this case, some PLAs chain couples cannot react with TAIC, forming cross-linking structures to prevent them from decoupling in the melt. However, for the blend prepared by melt-blending of pre-cross-linked PLLA and PDLA with 0.1 wt% TAIC and 0.3 wt% DCP (denoted as c-PLLA and c-PDLA, respectively), no obvious difference in the melt stability can be observed as compared with the un-cross-linked PLLA/PDLA blend. These results further confirm that the selective cross-linking of the mobile hetero-chiral PLAs chain couples is of great benefit to improving the melt stability, but the formation of cross-linked structure between homo-chiral PLA chains has no apparent influence on the melt stability.

From above considerations, it is clear that sc crystallites form rapidly during the blending process, followed by a slight cross-linking of mobile PLLA and PDLA chain couples in their amorphous phase. These selectively cross-linked chain couples play a vital role in enhancing the melt stability. Because the chain couples in the sc crystallites obtained from linear PLAs can be regard as zippers,[26] formation of a few cross-linking points at both ends of each chain couple could not only prevent it from completely unzipping after melting but also promote the two crystallizable segments between the cross-linking points interact and pack together in a side-by-side fashion upon subsequent cooling, thus endowing the obtained sc-PLA with an excellent ability to reassemble sc crystallites after melting and recrystallization. The role of the

selectively cross-linked chain couples on the enhancement in the melt stability of sc crystallites can be depicted by a simplified schematic shown in Scheme 2.

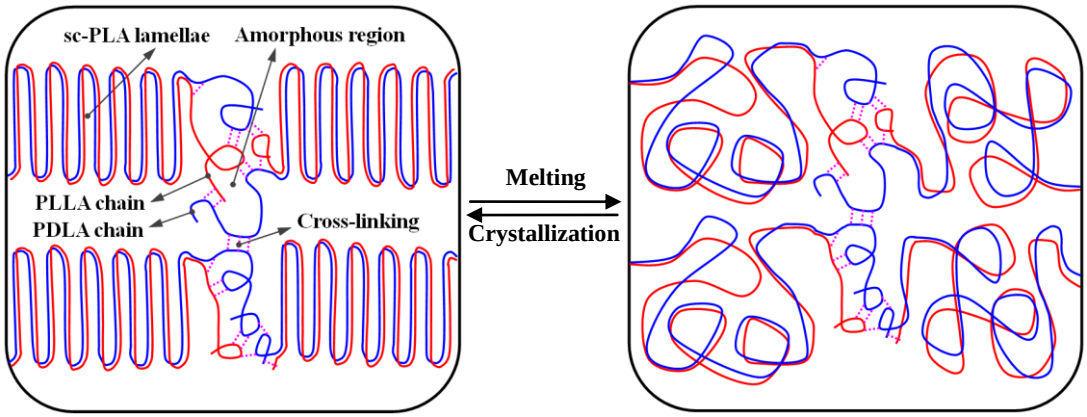

Scheme 2. A schematic representation showing the well-stereocomplexed PLAs with good melt-stability and excellent recrystallization ability.

3.3 Thermomechanical Properties

To highlight the importance of improving melt stability of PLLA/PDLA blend in practical applications, injection molded PLLA/PDLA blend with and without 0.5 wt% TAIC were prepared after melt-blending and their heat resistance was analyzed with DMA. For comparison, pure PLLA was also processed with the same procedure. All the injection molded samples have the same high level of crystallinity (40-45%) but different crystalline structures (Figure 10a). Evolution of storage modulus with the temperature for each sample is shown in Figure 10b. Clearly, the storage modulus of PLLA with 100 % hc crystallites drops considerably above the glass transition temperature (T_g) and no effective resistance to deformation is available with further increasing temperature up to $T_{m,hc}$. For PLLA/PDLA blend with 25 % hc crystallites and

75% sc crystallites, although the presence of sc crystallites can enhance the heat resistance between T_g and $T_{m,hc}$, the storage modulus is almost the same as that in PLLA when the temperature exceeds $T_{m,hc}$. However, for PLLA/PDLA blend with 100% sc crystallites, the value of G' at 200 ℃ is also comparable to that for PLLA at 94 ℃ and that for PLLA/PDLA blend at 149 ℃, indicating that excellent melt stability is a prerequisite for achieving pure sc crystallites and resulting high heat resistance in melt-process sc-PLA products.

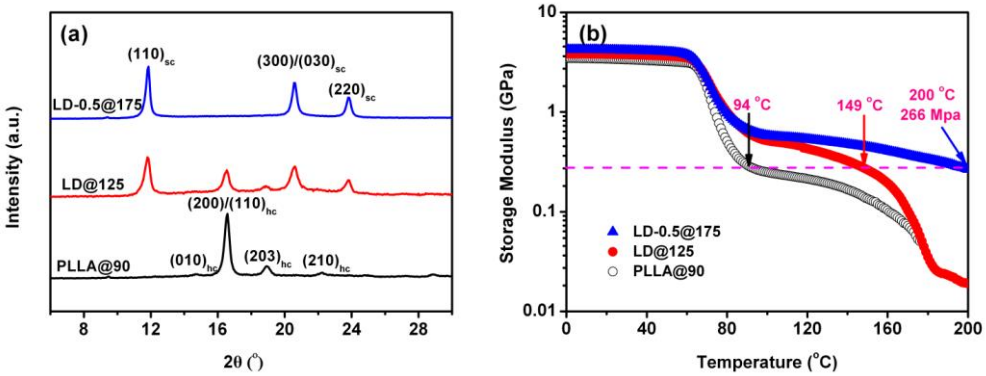

Figure 10. (a) WAXD profiles and (b) storage modulus (G') vs. temperature curves of injection molded PLLA, PLLA/PDLA blend, and PLLA/PDLA blend with 0.5 wt% TAIC.

4. Conclusions

In conclusion, we demonstrate a facile strategy to fabricate pure sc-PLA with good melt stability from linear high-molecular-weight PLLA and PDLA through selective cross-linking of mobile PLLA/PDLA chain couples in the amorphous phase of sc crystallites during the melt-blending process. The exclusive cross-linking could not only introduce abundant cross-linking points at the ends of the chain couples to prevent them from completely decoupling upon melting but also promote long crystallizable PLAs segments pack together in a side-by-side

manner upon subsequent cooling, thus endowing the obtained sc-PLA with an impressive ability to re-form sc crystallites from melt. Moreover, the formation of sc crystallites by melting and recrystallization is perfectly reversible in several thermal cycles. More importantly, the injection molded PLA article with 100% sc crystallites has been successfully prepared from cross-linked PLLA/PDLA blend and its outstanding heat resistance at the temperatures higher than the melting temperature of hc crystallites has been highlighted. We believe that this work could open a promising way toward industrial-scale fabrication of high-performance PLA products using conventional melt-processing equipments.

Acknowledgements: This work was supported by National Natural Science Foundation of China (51121001, 21034005) and China Postdoctoral Science Foundation (2013M530399).

Notes and references:

1. M. M. Reddy, S. Vivekanandhan, M. Misra, S. K. Bhatia and A. K. Mohanty, *Prog Polym Sci*, 2013, **38**, 1653-1689.
2. M. J. L. Tschan, E. Brule, P. Haquette and C. M. Thomas, *Polym Chem*, 2012, **3**, 836-851.
3. K. M. Nampoothiri, N. R. Nair and R. P. John, *Bioresour Technol*, 2010, **101**, 8493-8501.
4. J. W. Rhim, H. M. Park and C. S. Ha, *Prog Polym Sci*, 2013, **38**, 1629-1652.
5. L. T. Lim, R. Auras and M. Rubino, *Prog Polym Sci*, 2008, **33**, 820-852.
6. R. M. Rasal, A. V. Janorkar and D. E. Hirt, *Prog Polym Sci*, 2010, **35**, 338-356.

7. G. Stoclet, R. Seguela, J. M. Lefebvre, S. Li and M. Vert, *Macromolecules*, 2011, **44**, 4961-4969.

8. S. Saeidlou, M. A. Huneault, H. B. Li and C. B. Park, *Prog Polym Sci*, 2012, **37**, 1657-1677.

9. K. A. Athanasiou, G. G. Niederauer and C. M. Agrawal, *Biomaterials*, 1996, **17**, 93-102.

10. N. A. Weir, F. J. Buchanan, J. F. Orr, D. F. Farrar and A. Boyd, *Biomaterials*, 2004, **25**, 3939-3949.

11. S. R. Andersson, M. Hakkarainen, S. Inkinen, A. Sodergard and A. C. Albertsson, *Biomacromolecules*, 2010, **11**, 1067-1073.

12. D. Brizzolara, H. J. Cantow, K. Diederichs, E. Keller and A. J. Domb, *Macromolecules*, 1996, **29**, 191-197.

13. H. Tsuji, *Macromol Biosci*, 2005, **5**, 569-597.

14. H. Tsuji and Y. Ikada, *Polymer*, 1999, **40**, 6699-6708.

15. X. W. Zhang, R. Nakagawa, K. H. K. Chan and M. Kotaki, *Macromolecules*, 2012, **45**, 5494-5500.

16. P. Purnama and S. H. Kim, *Macromolecules*, 2010, **43**, 1137-1142.

17. M. Fujita, T. Sawayanagi, H. Abe, T. Tanaka, T. Iwata, K. Ito, T. Fujisawa and M. Maeda, *Macromolecules*, 2008, **41**, 2852-2858.

18. B. Na, J. Zhu, R. H. Lv, Y. H. Ju, R. P. Tian and B. B. Chen, *Macromolecules*, 2014, **47**, 347-352.

19. R. Y. Bao, W. Yang, W. R. Jiang, Z. Y. Liu, B. H. Xie, M. B. Yang and Q. Fu, *Polymer*, 2012, **53**, 5449-5454.

20. H. Tsuji and S. Yamamoto, *Macromol Mater Eng*, 2011, **296**, 583-589.

21. K. Nagahama, R. Aoki, T. Saito, T. Ouchi, Y. Ohya and N. Yui, *Polym Chem*, 2013, **4**, 1769-1773.

22. Y. He, Y. Xu, J. Wei, Z. Y. Fan and S. M. Li, *Polymer*, 2008, **49**, 5670-5675.

23. H. Tsuji and Y. Ikada, *Macromolecules*, 1993, **26**, 6918-6926.

24. K. Masutani, S. Kawabata, T. Aoki and Y. Kimura, *Polym Int*, 2010, **59**, 1526-1530.

25. K. Fukushima, Y. H. Chang and Y. Kimura, *Macromol Biosci*, 2007, **7**, 829-835.

26. T. Biela, A. Duda and S. Penczek, *Macromolecules*, 2006, **39**, 3710-3713.

27. J. Shao, J. R. Sun, X. C. Bian, Y. Cui, G. Li and X. S. Chen, *J Phys Chem B*, 2012, **116**, 9983-9991.

28. T. Isono, Y. Kondo, I. Otsuka, Y. Nishiyama, R. Borsali, T. Kakuchi and T. Satoh, *Macromolecules*, 2013, **46**, 8509-8518.

29. N. Yui, P. J. Dijkstra and J. Feijen, *J Makromol Chem,* 1990, **191**, 481-488.

30. K. Fukushima, Y. Furuhashi, K. Sogo, S. Miura and Y. Kimura, *Macromol Biosci*, 2005, **5**, 21-29.

31. H. Ajiro, Y. J. Hsiao, H. T. Tran, T. Fujiwara and M. Akashi, *Macromolecules*, 2013, **46**, 5150-5156.

32. C. Lavilla, E. Gubbels, A. M. de Ilarduya, B. A. J. Noordover, C. E. Koning and S. Munoz-Guerra, *Macromolecules*, 2013, **46**, 4335-4345.

33. H. Tsuji, M. Nakano, M. Hashimoto, K. Takashima, S. Katsura and A. Mizuno, *Biomacromolecules*, 2006, **7**, 3316-3320.

34. H. Z. Liu, F. Chen, B. Liu, G. Estep and J. W. Zhang, *Macromolecules*, 2010, **43**, 6058-6066.

35. Y. Liu, J. Sun, X. Bian, L. Feng, S. Xiang, B. Sun, Z. Chen, G. Li and X. Chen, *Polym Degrad Stabil*, 2013, **98**, 844-852.

36. T. M. Quynh, H. Mitomo, N. Nagasawa, Y. Wada, F. Yoshii and M. Tamada, *Eur Polym J*, 2007, **43**, 1779-1785.

37. J. Zhang, K. Tashiro, H. Tsuji and A. J. Domb, *Macromolecules*, 2008, **41**, 1352-1357.

38. S. L. Yang, Z. H. Wu, W. Yang and M. B. Yang, *Polym Test*, 2008, **27**, 957-963.

39. M. D'Haese, F. Langouche and P. Van Puyvelde, *Macromolecules*, 2013, **46**, 3425-3434.